

# Computational Analysis of Negative and Positive Allosteric Modulator Binding and Function in Metabotropic Glutamate Receptor 5 (In)Activation

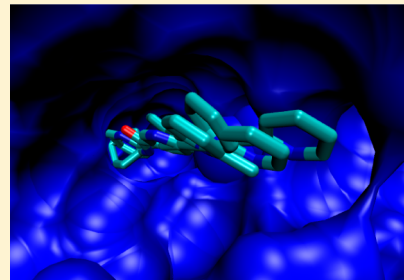
James A. R. Dalton,<sup>†</sup> Xavier Gómez-Santacana,<sup>‡,†</sup> Amadeu Llebaria,<sup>‡</sup> and Jesús Giraldo\*,<sup>†</sup>

<sup>†</sup>Laboratory of Molecular Neuropharmacology and Bioinformatics, Institut de Neurociències and Unitat de Bioestadística, Universitat Autònoma de Barcelona, 08193 Bellaterra, Barcelona, Spain

<sup>‡</sup>Laboratory of Medicinal Chemistry, Department of Biomedicinal Chemistry, Institut de Química Avançada de Catalunya (IQAC-CSIC), Jordi Girona 18-26, 08034 Barcelona, Spain

## S Supporting Information

**ABSTRACT:** Metabotropic glutamate receptors (mGluRs) are high-profile G-protein coupled receptors drug targets because of their involvement in several neurological disease states, and mGluR5 in particular is a subtype whose controlled allosteric modulation, both positive and negative, can potentially be useful for the treatment of schizophrenia and relief of chronic pain, respectively. Here we model mGluR5 with a collection of positive and negative allosteric modulators (PAMs and NAMs) in both active and inactive receptor states, in a manner that is consistent with experimental information, using a specialized protocol that includes homology to increase docking accuracy, and receptor relaxation to generate an individual induced fit with each allosteric modulator. Results implicate two residues in particular for NAM and PAM function: NAM interaction with W785 for receptor inactivation, and NAM/PAM H-bonding with S809 for receptor (in)activation. Models suggest the orientation of the H-bond between allosteric modulator and S809, controlled by PAM/NAM chemistry, influences the position of TM7, which in turn influences the shape of the allosteric site, and potentially the receptor state. NAM-bound and PAM-bound mGluR5 models also reveal that although PAMs and NAMs bind in the same pocket and share similar binding modes, they have distinct effects on the conformation of the receptor. Our models, together with the identification of a possible activation mechanism, may be useful in the rational design of new allosteric modulators for mGluR5.



## INTRODUCTION

Glutamate is the most significant excitatory neurotransmitter in the CNS and is involved in several neurological disorders such as chronic pain, schizophrenia, Alzheimer's, and epilepsy.<sup>1–4</sup> Glutamate activates two different kinds of receptors: fast-acting ionotropic cation channels responsible for neurological ionic transmission,<sup>5</sup> and slower-acting metabotropic glutamate (mGlu) G-protein coupled receptors (GPCRs) responsible for more sustained modulation of pre- and postsynaptic neuronal activity.<sup>6,7</sup> The mGlu receptor (mGluR) family belongs to the GPCR Class C family and contains eight receptor subtypes.<sup>8</sup> All members form stable disulphide-linked dimers,<sup>9</sup> with each monomer containing an extracellular Venus flytrap domain (VFT), which contains the orthosteric glutamate binding site (Figure 1). The heptahelical transmembrane (7TM) domain contains the allosteric binding site and is analogous to the 7TM domain of Class A GPCRs.<sup>8,10</sup> The 7TM domain of mGluRs is linked to the VFT domain by a unique cysteine-rich region (Figure 1).

The allosteric modulation of mGluRs is an active area of drug research because this strategy offers some advantages over the more conventional targeting of the receptor's orthosteric site in the VFT domain.<sup>11–13</sup> These advantages include better

receptor subtype selectivity due to a greater number of differences across the family's allosteric sites compared to their orthosteric sites, as well as a reduced risk of receptor oversensitization, as strict allosteric modulators (those with no intrinsic agonist activity) only modulate the natural response to the endogenous ligand and do not activate the receptor on their own. This means the spatial and temporal effect of glutamate is maintained intact, which is a distinct therapeutic advantage. However, orthosteric ligands also have their own therapeutic advantages such as better solubility, reduced interaction with other brain proteins, and no turnover by CYP450.<sup>11</sup> Of the mGluRs, mGluR5 is a particularly attractive target for allosteric modulation because its stimulation can potentially be a therapy for schizophrenia<sup>14</sup> while its inhibition can potentially treat anxiety,<sup>15</sup> depression,<sup>16</sup> and pain.<sup>17</sup> However, as no crystal structure data are currently available for the 7TM domain of mGluR5, nor of any other Class C GPCR,<sup>18</sup> the structural analysis of allosteric modulator binding is only possible through homology modeling from distantly related Class A GPCRs. This is particularly difficult because despite a similar structural

Received: February 27, 2014

Published: May 3, 2014

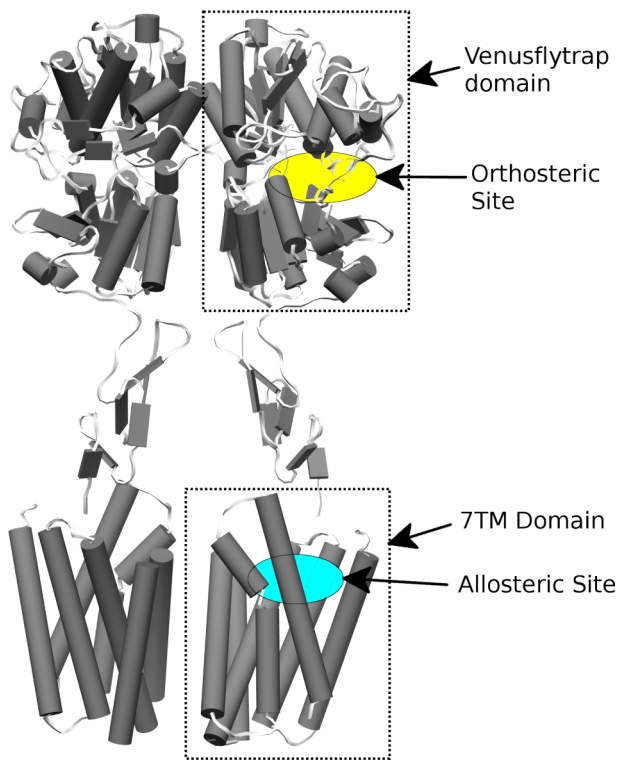


**Figure 1.** Representation of an mGluR5 homodimer. Helices are shown as cylinders and strands as planks.

fold, sequence identity between these two families is  $\leq 20\%$  in the 7TM domain,<sup>19</sup> a level typically described as the twilight zone, and well-known to result in modeling and docking errors.<sup>20,21</sup>

Here, we use a previously developed modeling protocol, specifically designed for homology modeling low sequence identity targets with ligand-induced conformational change,<sup>22</sup> for modeling the 7TM domain of mGluR5 with a collection of diverse allosteric modulators. We chose not to model the extracellular domain of mGluR5 as including this significantly increases the modeling complexity, and as the 7TM domain is fully functional and responsive as an independent unit,<sup>10</sup> the modeling of this domain in isolation is a legitimate approach for investigating 7TM domain allosteric modulation. However, this does mean that the mutual cooperativity effects between VFT and 7TM domains are not explicitly included in the model. The interaction between these two domains has been considered previously under a mathematical modeling framework<sup>23,24</sup> but is beyond the scope of our current approach. Here, our modeling protocol uses specialized software in a stepwise manner, combined with manual editing where necessary, and proceeds as follows: multiple sequence alignment incorporating structural data, flexible ligand–ligand superposition, protein–ligand modeling with spatial restraints, flexible docking with receptor conformational change including side-chain and backbone flexibility, clustering of models, and postmodeling geometrical analysis. Homology-guided docking utilizes information from related protein–ligand crystal structures and has been shown to improve docking accuracy in homology models,<sup>22</sup> and is relevant here in terms of predicting protein–ligand interactions in a Class C GPCR based on Class A GPCR protein–ligand interactions, where the allosteric site of mGluR5 is considered equivalent to the orthosteric site of Class A GPCRs.<sup>8,10</sup> In addition to docking, allowing for full

receptor flexibility on an individual basis is necessary for generating an induced fit and establishing the effect of each ligand on protein structure.<sup>22</sup>

Specifically, we investigate the effect eight different, previously characterized, allosteric modulators (four positive<sup>25–27</sup> and four negative<sup>25,28,29</sup>) have when docked into models of the 7TM domain of mGluR5, in order to identify the common and differential aspects of binding and receptor conformation. This in turn can potentially be used to infer a common mechanism of allosteric (in)activation. In order to increase the accuracy of docking and receptor structure, two different states of mGluR5–7TM are independently modeled, in active and inactive states from multiple templates. The active state of mGluR5 is primarily used for positive allosteric modulator (PAM) docking, while the inactive state is primarily used for negative allosteric modulator (NAM) docking, although “crossover” docking is also utilized to determine the effect on the receptor when a NAM is docked into the active state, or vice versa. Although homology models of mGluR5 have been previously published, they have only been generated from one or two Class A GPCR template(s) in the inactive state,<sup>27,29–31</sup> even when used for PAM docking,<sup>27</sup> with one group attempting to generate an “activelike” state from normal-mode analysis of rhodopsin.<sup>32</sup> However, these models have generally been inconclusive in terms of the molecular mechanism responsible for allosteric modulation because of the absence of an active-state model (no active Class A GPCR structures have been available until recently; e.g., see refs 33 and 34), as well as deficiencies in docking frequently encountered with homology models.<sup>21,22</sup> We seek to address some of these issues through multiple-state, multiple-template homology modeling, combined with homology-guided docking and extensive receptor optimization for induced fit, with subsequent comparison of PAM and NAM binding, which is as consistent as possible with available mutational data.<sup>1,8,27,35,36</sup>

## MATERIALS AND METHODS

**Multiple Sequence Alignment.** A multiple sequence alignment between the eight members of the mGluR family (1–8) and 13 Class A GPCR sequences with corresponding structures in the Protein Data Bank<sup>37</sup> (PDB ids: 3UON, 4DAJ, 3RZE, 3PBL, 2Y00, 3SN6/2RH1, 4GRV, 3OE0, 2YDV, 3VG9, 3V2Y, 1L9H, 3DQB) was generated with ProMALS-3D,<sup>38</sup> a sequence–structure alignment technique, and then manually edited to achieve optimal accuracy with respect to TM helices.

**Ligand Selection and Construction.** Eight allosteric modulators (four NAMs and four PAMs) were chosen (see Figure 2) based on structural variety and available experimental and mutational data. The NAMs, CHPyEPC, 1,4-bisPEB, MPEP, and 1,3-bisPEB,<sup>25,28,29</sup> and PAMs, CHPhEPC, VU0403602, VU0405386, and CIDPPB,<sup>25–27</sup> were built *de novo* with Maestro<sup>39</sup> and minimized in the OPLS2005 force field.<sup>40</sup>

**Ligand Superposition and Template Preparation.** The crystal structure ligands of inactive-state GPCRs, 2RH1, 3V2Y, and 3PBL, were superimposed by aligning their respective protein structures with CHIMERA.<sup>41</sup> The four selected NAMs (see above) and PAM CHPhEPC were individually superimposed onto the three aligned template antagonists (from 2RH1, 3V2Y, 3PBL) in a flexible manner using OMEGA<sup>42</sup> and ROCS.<sup>43</sup> In the same way, the four selected PAMs and NAM CHPyEPC were individually aligned onto the agonist of the crystal structure of active-state GPCR: 3SN6. This process

created four modified GPCR protein structures (2RH1, 3V2Y, 3PBL, 3SN6) each containing respective bound mGluR5 allosteric modulators that would serve as templates for modeling the mGluR5 protein. Before the subsequent modeling step, and only if necessary, the orientation of allosteric modulator in its respective template structure(s) was manually optimized with CHIMERA to minimize clashes with semi-conserved (e.g., V2.61 of D3R, I7.36 and N7.39 of B2AR, Ballesteros–Weinstein indexing<sup>44</sup>) and conserved side chains (e.g., W6.48 and F6.51 of B2AR). This was intended to increase docking accuracy as well as maintain the orientation of (semi)conserved side chains during mGluR5 modeling.

**Homology Modeling and Initial Docking.** Based on the multiple sequence alignment, MODELER<sup>45</sup> v9.11 was used for homology modeling of the 7TM domain of mGluR5 and transferring the respective allosteric modulator (NAM or PAM) from template into mGluR5. The inactive state of mGluR5 was modeled from multiple templates:  $\beta$ -2-adrenergic receptor (PDB id: 2RH1), sphingosine 1-phosphate receptor 1 (PDB id: 3V2Y), and dopamine D3 receptor (PDB id: 3PBL), each containing the respective mGluR5 allosteric modulator. In addition, the extracellular loop-2 (ECL2) of the neurotensin receptor (PDB id: 4GRV) was excised and used for modeling ECL2 of mGluR5, as predictions suggested higher structural similarity in this area compared to other templates. ECL2 is known to interact with ligands in Class A GPCRs so was considered important in mGluR5 also. The active state of mGluR5 was modeled from two templates: the active state of the  $\beta$ -2-adrenergic receptor (PDB id: 3SN6), containing the respective mGluR5 allosteric modulator, and the neurotensin receptor (PDB id: 4GRV) for modeling ECL2. Using this protocol, five inactive-state models of mGluR5 were generated with NAMs CHPyEPC, 1,4-bisPEB, MPEP, 1,3-bisPEB, and with PAM CHPheEPC. Likewise, five active-state models were generated with PAMs CHPheEPC, VU0403602, VU0405386, and CIDPPB, and with NAM CHPyEPC.

**Protein and Docking Refinement.** Each MODELER-generated mGluR5 model with bound allosteric modulator was energetically relaxed with ROSETTA v3.4 in an implicit membrane.<sup>46</sup> This protocol incorporates full flexibility in protein side chains and backbone, as well as ligand conformation and orientation. From a single starting model, ROSETTA relaxation generated  $> 1000$  alternative protein–ligand conformations, which were subsequently clustered with a root mean square deviation (RMSD)  $< 2 \text{ \AA}$ . The final optimized model was selected based on the lowest ROSETTA energy score and belonging to the largest cluster. In this way, 10 fully optimized mGluR5-modulator models were generated.

**Measurement of Allosteric Site.** The geometrical properties of the allosteric site in each mGluR5-modulator model were assessed with POVME<sup>47</sup> using default parameters. The center of the allosteric site in each model was defined as the center of the bound allosteric modulator.

## RESULTS

Eight allosteric modulators of mGluR5, four PAMs and four NAMs, were docked into homology models of the 7TM domain of mGluR5 in active and inactive states, respectively, using a homology-guided, fully flexible, induced-fitting protocol that has been shown to be more accurate than conventional “blind” docking into homology models.<sup>22</sup> The eight allosteric modulators include the NAMs MPEP, CHPyEPC, 1,3-bisPEB, and 1,4-bisPEB,<sup>25,28,29</sup> and PAMs CIDPPB, CHPheEPC,

VU0403602, and VU0405386<sup>25–27</sup> (see Figure 2). In line with their inhibitory function, each NAM was docked into its

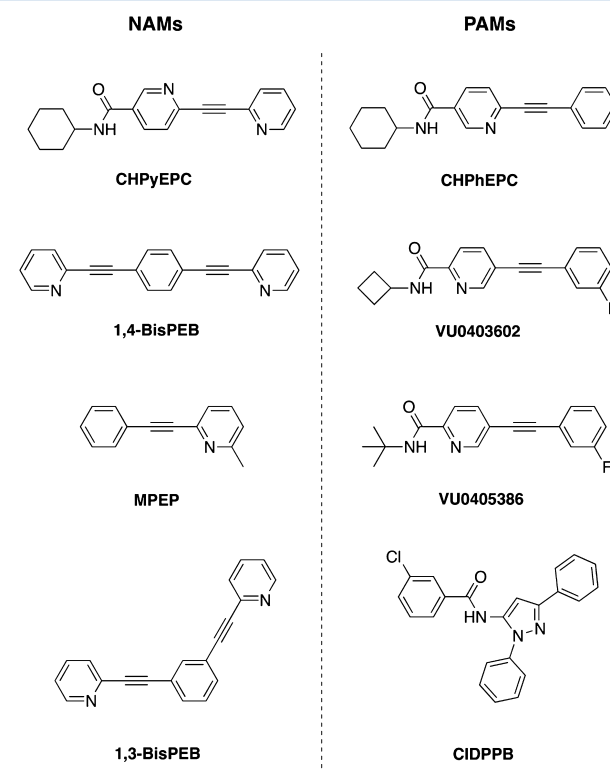


**Figure 2.** Eight allosteric modulators docked into models of mGluR5. CHPyEPC and CHPheEPC only differ in one atom position. MPEP and VU0405386 are considered 2-ring systems, which are distinguishable from the other  $\geq 3$ -ring systems.

own individual inactive state of mGluR5, while each PAM, in line with their stimulatory function, was docked into an individual active state. As a further comparison, the NAM CHPyEPC was also docked into an active state of mGluR5, and the PAM: CHPheEPC docked into an inactive state, to look for induced changes in the receptor. These two allosteric modulators are of particular interest as they differ in only one atom position, where the terminal pyridine ring in the NAM is converted into a phenyl ring in the PAM (see Figure 2). Therefore observing how these two allosteric modulators interact with active and inactive states of the receptor was considered particularly relevant for understanding the allosteric mechanism.

The inactive state of the 7TM domain of mGluR5 was modeled from multiple Class A GPCR templates in their inactive state (sequence alignment shown in Supporting Information (SI) Figure 1). This protocol provides the best possible sequence and structural coverage across mGluR5, as well as providing ligand variation for homology-guided docking. The three templates for modeling the inactive 7TM domain are as follows:  $\beta$ -2-adrenergic receptor (B2AR; PDB id, 2RH1), sphingosine 1-phosphate receptor 1 (S1PR1; PDB id, 3V2Y), and dopamine D3 receptor (D3R; PDB id, 3PBL), as well as a fourth template for exclusively modeling extracellular loop-2 (ECL2): the  $\beta$ -hairpin loop from neurotensin receptor (NTSR1; PDB id, 4GRV). In terms of structural features, all three 7TM templates closely superimpose with an RMSD  $< 2 \text{ \AA}$  (see Figure 3A), providing a complementary scaffold for

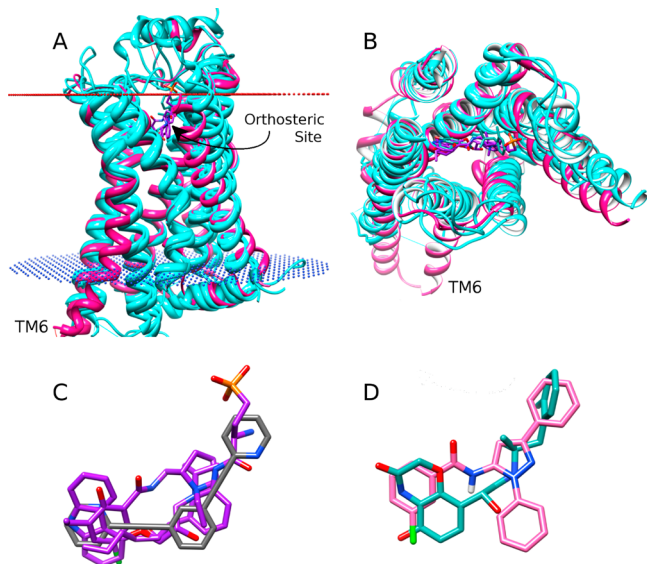


**Figure 3.** Overview of template Class A GPCR structures used in modeling mGluR5. (A) Three inactive structures (in cyan),  $\beta$ -2-adrenergic receptor (B2AR), sphingosine 1-phosphate receptor 1 (S1P1R), and dopamine D3 receptor (D3R), and active structure (in pink),  $\beta$ -2-adrenergic receptor (B2ARa), superimposed with CHIMERA,<sup>41</sup> (B) Same superimposition as in A, shown from the top extracellular point of view. The respective antagonists (in purple) and agonist (in teal) closely superimpose within the aligned orthosteric binding site. (C) Superimposition of NAM 1,3-bisPEB (in gray) on antagonists of B2AR, S1P1R, and D3R (in purple). (D) Superimposition of PAM CIDPPB (in pink) on the agonist of B2ARa (in teal).

modeling mGluR5. All templates have a low sequence identity with respect to mGluR5: D3R, 20% identity; B2AR and S1P1R, 16%. However, by combining different sequences, overall modeling coverage is improved, e.g., regarding TM5, where the helix content and length in mGluR5 resembles that of S1P1R, which contains a tighter helical turn than B2AR or D3R (prior to the conserved LLXLS sequence motif, see sequence alignment in SI Figure 1). In addition to protein structure, all three co-crystallized antagonists guide docking of mGluR5 NAMs. An example is shown in Figure 3C where 1,3-bisPEB is superimposed onto the antagonists of B2AR, S1P1R, and D3R to maximize geometric and chemical overlap. This is possible because the orthosteric binding sites in the templates, as well as their ligands, closely correlate (Figure 3B). Indeed, it is this aspect of the highly conserved 7TM-fold that serves as the basic premise of homology modeling: that the orthosteric binding site in Class A GPCRs is structurally homologous to the allosteric site in mGluR5<sup>8,10</sup> and permits homology-guided docking of allosteric modulators.

The active state of the 7TM domain of mGluR5 was modeled based on two templates: the active state of the B2ARa (PDB id, 3SN6), which was the only active GPCR structure with a bound G-protein available at the time, and NTSR1 (PDB id, 4GRV), which was used for modeling ECL2. Compared to the inactive state of B2AR, the active state B2ARa shows a significantly different conformation on the intracellular side, particularly in relation to TM6, which bends outward to enable binding of the G-protein, but also in relation to TM7, which partially unravels and shortens in length (see Figure 3A,B). However, there is less difference in the orthosteric binding site between inactive and active states of

B2AR (Figure 3B), which perhaps means it is not the most representative of GPCR active states. However, despite this, certain structural features make it suitable for modeling mGluR5, such as its co-crystallized agonist, which closely matches the position of antagonists in inactive GPCR structures (Figure 3B) and guides the docking of PAMs in the active state. An example is shown in Figure 3D, where CIDPPB is superimposed onto the B2ARa agonist, providing a satisfactory geometrical fit and binding-site complementarity, despite differences in ligand chemical groups. Although an active-state structure of rhodopsin is available,<sup>33</sup> because of the lack of bound G-protein, its internal ECL2 and covalently bound ligand (retinal), both features unusual with respect to receptors that recognize diffusible ligands, it was deemed inappropriate for modeling mGluR5.

Some mutational studies of mGluR5, together with construction of homology models, have previously identified several residues involved in NAM and PAM binding and functionality.<sup>27,35,36</sup> These studies use different sequence alignments from ours between mGluR5 and B2AR, with the main differences lying in TM2, TM4, and TM5 (see SI Figure 2). These ultimately result in different models, mostly affecting these three helices. However, as the allosteric site of mGluR5 is mostly composed of TM3, TM5, TM6, and TM7<sup>8</sup> (Figure 4), as far as we can tell, previous models are relatively similar to ours in this area, although some differences exist such as in the position of residues in TM5. However, only a comparison of inactive states is possible as, to our knowledge, ours is the first published homology model of active mGluR5. To illustrate how our models are in accordance with previously published mutational data,<sup>27,36</sup> residues in contact distance (protein–ligand distance < 3.5 Å) with docked NAMs: MPEP and 1,3-BisPEB and docked PAMs VU0403602 and VU0405386 (see Figure 2) are listed and compared with experimental information (Table 1). In each of the four models (two inactive with NAMs and two active with PAMs), the vast majority of modulator-contacting residues are known to be functionally significant, although no data are available for residues located on TM2, TM4, and ECL2. Figure 4A shows the inactive model of mGluR5, with residues making direct interactions with NAMs displayed. The majority of these residues are known to be involved in NAM function.

Furthermore, by modeling active and inactive states with docked PAMs and NAMs, respectively, it is possible to see which residues are involved in both forms of allosteric modulation and which residues are involved in just one or the other. First, Table 2 and Figure 4B show residues which are common among PAMs and NAMs, including residues which are common among all eight docked modulators, as well as residues which are common among only a subset. A cluster of residues on TM3 (I651, G652, P655), as well as Y792 on TM6, and V806 and S809 on TM7, form the foundation of interactions with all eight modulators. Other notable residues only form interactions among a subset, e.g., F788 on TM6 is present in all interactions except with the 2-ring PAM VU0405386, while N747 on TM5 is present in all 3-ring and 4-ring modulators but absent in interactions with both 2-ring modulators MPEP and VU0405386. This can be explained by the fact that 2-ring modulators do not reach as far into the pocket as 3-ring or 4-ring modulators, with N747 predicted to occupy a position at the far end of the pocket.

Second, Table 3 and Figure 4D show the residues that only interact with NAMs but not PAMs, or vice versa. The most

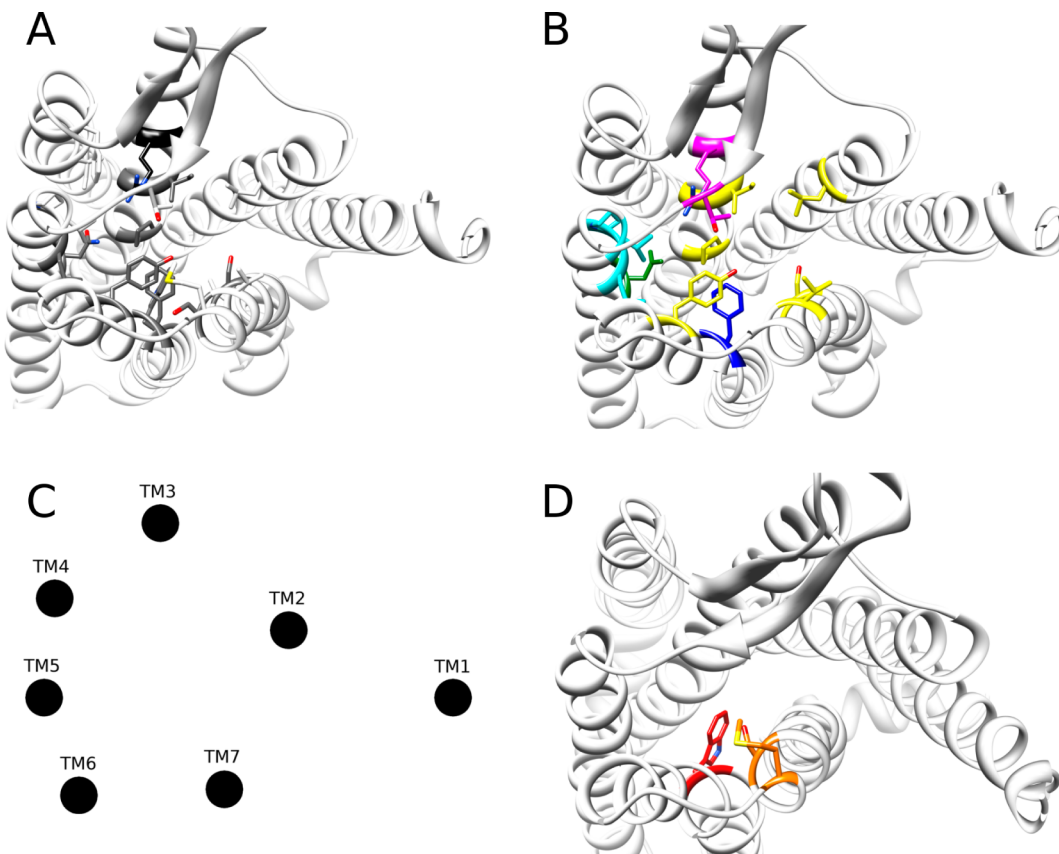


**Figure 4.** mGluR5 residues involved in NAM and PAM binding. (A) Inactive model of mGluR5, with residues making direct contacts with NAMs displayed ( $<3.5\text{ \AA}$ ). Those highlighted in dark gray have been shown by experiment to be functionally significant. Those highlighted in black have been shown to be experimentally insignificant. Those in light gray have no corresponding experimental data. (B) Model of mGluR5 showing the common residues directly involved ( $<3.5\text{ \AA}$ ) in PAM and NAM binding. Residues highlighted in yellow bind all PAMs and NAMs; in green, bind all 3-ring NAMs (not MPEP) and all 3-ring PAMs (not VU0405386); in blue, bind all NAMs and all 3-ring PAMs (not VU0405386); in pink, bind all PAMs; in cyan, bind all 3-ring NAMs (not MPEP). (C) Representation of the 7TM helix arrangement. (D) Model of mGluR5 showing the residue that interacts with NAMs but not PAMs W785 (in red), and residues interacting with PAMs but not NAMs M802 and S805 (in orange).

significant interaction in this category is W785 on TM6, which is equivalent to the highly conserved W6.48 in Class A GPCRs and has been postulated to be involved in ligand binding and determination of receptor state.<sup>48–50</sup> Interestingly, in our models, this residue is only directly involved in NAM interactions and adopts a perpendicular orientation with respect to the membrane, pointing toward TM3. However, in PAM binding, as TM6 undergoes reorientation, W785 adopts a more tilted or horizontal orientation and points toward G748 on TM5, away from the binding site (see Figure 5). Interestingly, W785 has been shown to be experimentally significant in NAM functionality for both 1,3-bisPEB and MPEP,<sup>36</sup> but of less significance in PAM binding, with only a partial effect on VU0403602, none on VU0405386, and none on any of the other PAMs tested.<sup>27</sup> This suggests a role for W785 in the (in)activation of mGluR5 with a direct NAM interaction helping to stabilize the inactive state, and a tilted orientation favoring TM6 translocation and receptor activation. Conversely, residues that exclusively interact with PAMs only include M802 and S805, both of which are located on TM7 (see Figure 4D) and are perhaps indicative of a greater interaction between TM7 and PAMs. Indeed, experiments have shown that M802 facilitates PAM functionality but not NAM functionality.<sup>1,8</sup>

Perhaps the most significant result revealed by experiment, is the contribution of S809, localized on TM7, on both NAM and

PAM activity. The mutation S809A significantly reduces MPEP and 1,3-bisBEP potency<sup>36</sup> while also significantly decreasing PAM functionality, including VU0403602 and VU0405386, with the latter converted into a neutral modulator.<sup>27</sup> Both previous studies have reached the same conclusion, that an H-bond is formed between S809 and allosteric modulator and lost upon mutation.<sup>27,36</sup> However, the effect this residue and its potential H-bond have on the receptor state has yet to be elucidated. The results of modeling support the existence of an H-bond between S809 and both PAMs and NAMs in all receptor states (see Tables 1 and 2 and Figure 4B). Furthermore, different H-bond orientations appear to favor different positions of TM7 in active and inactive states, respectively. In the active state, the H-bond between PAM and S809 points toward TM3 (Figure 6D), orientating TM7 closer to TM3 and TM6. In the inactive state, the H-bond points toward TM2, moving TM7 away from TM3 and TM6 (Figure 6B). The reason for this change in orientation is due to the presence/absence of an electron-donating group (in this case a nitrogen atom) at the modulator's terminal ring. All docked NAMs contain a pyridine group in this position (Figure 2), which preferentially H-bonds with S809, while PAMs lack this group, instead containing a terminal phenyl ring (Figure 2), which is unable to make an H-bond with S809. Instead, in the case of PAMs, S809 forms an H-bond with the central pyridine or pyrazole ring, favoring a different orientation of TM7. This

**Table 1.** Residues<sup>a</sup> Predicted To Be within 3.5 Å of Four Docked Allosteric Modulators in mGluR5 in the Context of Available Functional Mutational Data Relevant to Those Specific Compounds<sup>27,36</sup>

Inactive State Residues in contact with NAM		Active State Residues in contact with PAM		Location
MPEP	1,3-BisPEB	VU0403602	VU0405386	
Leu 630	Leu 630	Leu 630	Leu 630	TM2
	Arg 648	Arg 648	Arg 648	TM3
Ile 651	Ile 651	Ile 651	Ile 651	TM3
Gly 652	Gly 652	Gly 652	Gly 652	TM3
Pro 655	Pro 655	Pro 655	Pro 655	TM3
Phe 712	Phe 712			TM4
	Thr 735	Thr 735	Thr 735	ECL2
	Val 740		Val 740	TM5
	Leu 744		Leu 744	TM5
	Asn 747	Asn 747		TM5
Trp 785	Trp 785			TM6
Phe 788	Phe 788	Phe 788		TM6
Tyr 792	Tyr 792	Tyr 792	Tyr 792	TM6
		MET 802		TM7
		Ser 805		TM7
Val 806	Val 806	Val 806	Val 806	TM7
Ser 809	Ser 809	Ser 809	Ser 809	TM7

<sup>a</sup>Residues highlighted in gray are confirmed by experiment to affect affinity/functionality of the allosteric modulator. Residues highlighted in black have been confirmed to not affect affinity/functionality (although this does not preclude their presence in the binding-site). No data are available for the other residues listed.

**Table 2.** Common Binding Residues (<3.5 Å to PAM/NAM) Identified among Eight Docked Allosteric Modulators in Active and Inactive States of mGluR5, Respectively

commonality	residues	location
present in all PAMs and NAMs (8/8)	Leu 630	TM2
	Ile 651	TM3
	Gly 652	TM3
	Pro 655	TM3
	Tyr 792	TM6
	Val 806	TM7
	Ser 809	TM7
present in all NAMs and all 3-ring PAMs (not VU0405386) (7/8)	Phe 788	TM6
present in all 3-ring NAMs (not MPEP) and all 3-ring PAMs (not VU0405386) (6/8)	Asn 747	TM5
present in all PAMs (4/8)	Arg 648	TM3
	Thr 735	ECL2
	Trp 785	TM6
present in all NAMs (4/8)	Val 740	TM5
Present in all 3-ring NAMs (not MPEP) (3/8)	Pro 743	TM5
	Leu 744	TM5

can be seen more clearly in the case of NAM CHPyEPC and PAM CHPhEPC. With the substitution of one atom, a pyridine group in CHPyEPC is converted into a phenyl group in CHPhEPC, a NAM is converted into a PAM, which causes a change in the direction of the H-bond with S809 and a different position of TM7 (Figure 6F).

**Table 3.** Differential Binding Residues (<3.5 Å to Ligand) Identified among Docked PAMs and Docked NAMs in Active and Inactive States of mGluR5, Respectively.

differential	residues	location
present in PAMs and 0 NAMs (2/8)	M802	TM7
	S805	TM7
present in NAMs and 0 PAMs (4/8)	W785	TM6

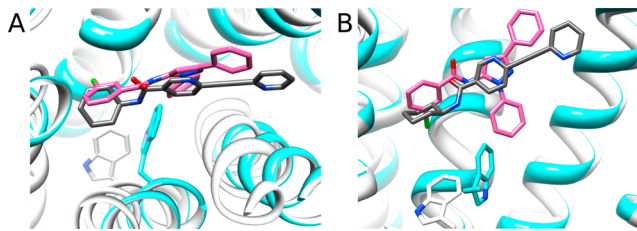


**Figure 5.** Comparison of W785 in the active (in light gray) and inactive states (in cyan) of mGluR5. (A) View from extracellular side and (B) side view from within the membrane. In the active state, W785 is tilted on its side and points away from the allosteric site and PAM CIDPPB, while, in the inactive state, W785 makes a direct interaction with NAM CHPyEPC.

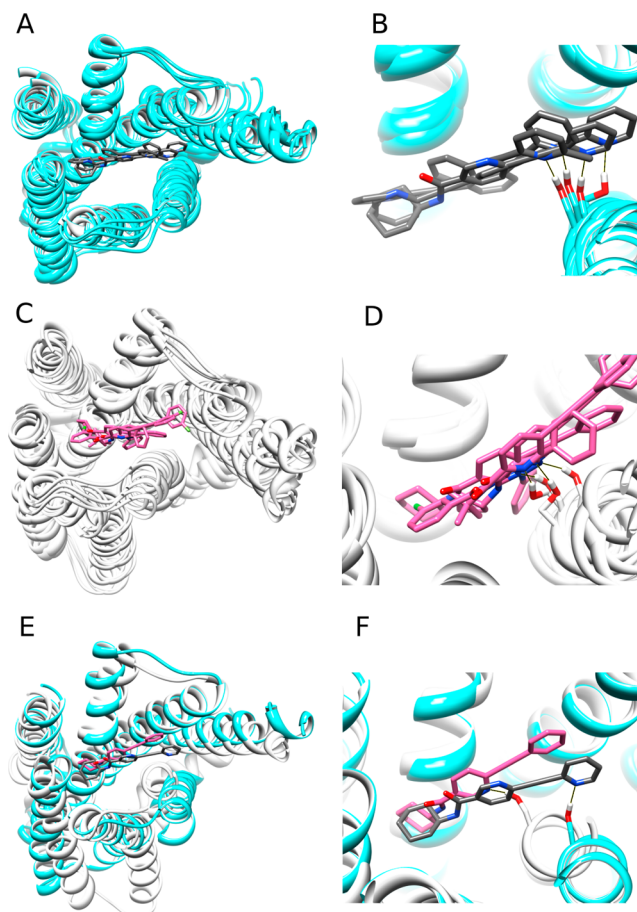


**Figure 6.** Comparison of PAM and NAM binding in active and inactive states of mGluR5. H-bonds between S809 and NAM/PAMs in black. (A and B) Inactive states of mGluR5 with docked NAMs (dark gray). (C and D) Active states of mGluR5 with docked PAMs (pink). (E and F) Comparison of PAM CHPhEPC (pink) and NAM CHPyEPC (dark gray) in active (light gray) and inactive (cyan) states, respectively.

An analysis of the overall geometrical shape of allosteric site in active and inactive states of mGluR5 is particularly revealing of the PAM/NAM effect, as calculated with POVME.<sup>47</sup> Overall, the PAM active models share similar geometrical features, specifically a “pinching” in the middle of the site between TM3 and TM7, as well as an “expansion” at the end of the pocket near TM4, TM5, and TM6. This combination of factors leads to an “hour-glass” shape (Figure 7A–D), although some

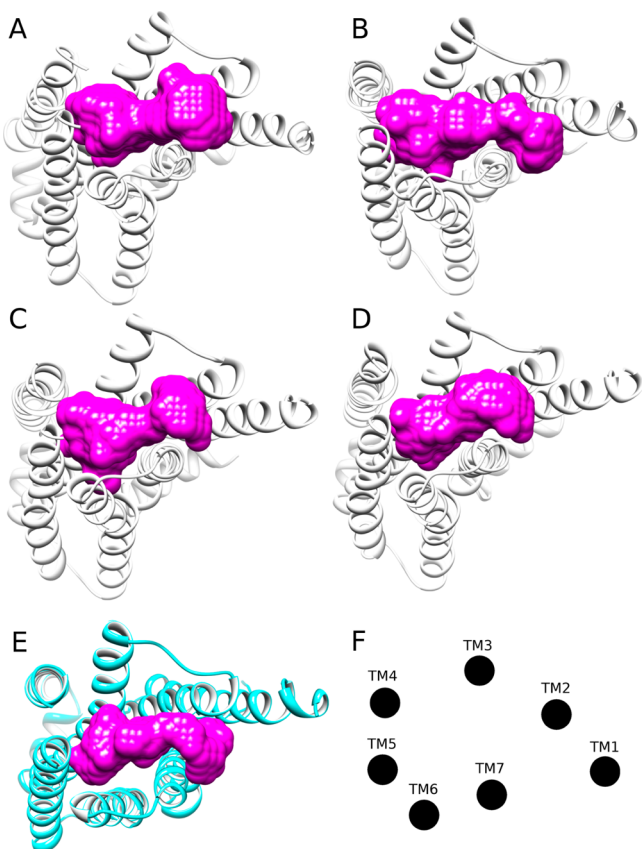


**Figure 7.** Effect of PAM binding on allosteric site of mGluR5, calculated with POVME.<sup>47</sup> (A–D) Active states of mGluR5 with PAMs CHPyEPC, CIDPPB, VU0405386, and VU0403602, respectively. Allosteric site shown as continuous purple volume. (E) Inactive (or intermediate) state of mGluR5 with PAM CHPyEPC. (F) Representative distribution of helices in mGluR5.

differences are apparent due to different induced fits. Interestingly, when the PAM CHPyEPC is docked into the inactive state of mGluR5, a pinching of the allosteric site is also observed, like in the active state, although some of the other features are less clear (Figure 7E). This may reflect an intermediate state between the inactive and active.

The NAM inactive states also share a common feature, which is different from that seen in the active state. In this instance, a clear “bulging” in the middle of the allosteric site between TM3 and TM7 is observed, as well as a narrowing at the end of the site near TM4, TM5, and TM6 (Figure 8A–D). This creates a “hand” shape, although some differences occur due to different induced fits. In addition, when the NAM CHPyEPC is docked into the active state of mGluR5, it elicits an effect on the receptor that resembles inactive models, which may represent an intermediate state.

Interestingly, the observed differences between inactive and active states in mGluR5 are more overt than in the B2AR and

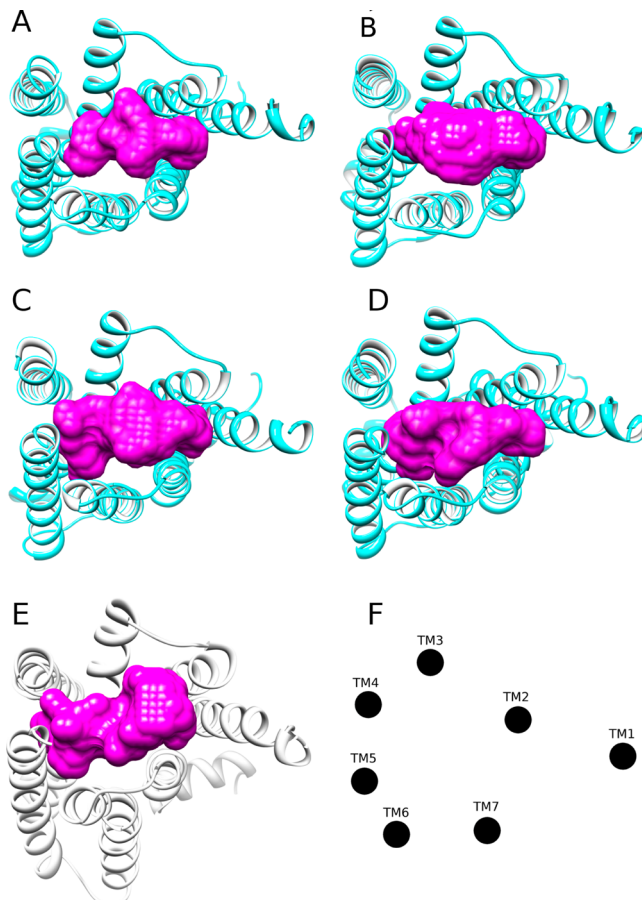


**Figure 8.** Effect of NAM binding on allosteric site of mGluR5, calculated with POVME.<sup>47</sup> (A–D) Inactive states of mGluR5 with NAMs CHPyEPC, MPEP, 1,3-bisPEB and 1,4-bisPEB, respectively. Allosteric site shown as continuous purple volume. (E) Active (or intermediate) state of mGluR5 with NAM CHPyEPC. (F) Representative distribution of helices in mGluR5.

B2AR structures (Figure 9A,B). This suggests that modeling, and in particular ROSETTA relaxation,<sup>46</sup> creates an induced fit suited to mGluR5. In support of these observed structural changes, recently published crystal structures of the inactive and active states of the Class A GPCR M2 muscarinic acetylcholine receptor (the active state was released after modeling was performed) reveal significant conformational shifts in the binding site upon agonist binding and receptor activation.<sup>51</sup> Among these changes include a shift of TM7 toward TM3, mediated by protein–agonist interactions that cause a restriction in the center of the binding site (Figure 9E,F). This mode of activation is reminiscent of that observed here in mGluR5. Furthermore, the different modeled states of mGluR5 closely superimpose onto the different states of the M2 muscarinic acetylcholine receptor (Figure 10). This suggests induced-fit modeling generates realistic structures, within the scope of currently known GPCR crystallized states.

## ■ DISCUSSION

In this study we present new models of mGluR5 in both inactive and active states, based on a manually edited multiple sequence alignment and carefully selected multiple structural templates. We flexibly dock NAMs and PAMs into both modeled states, a process which is guided by homology in a manner consistent with experimental information. From

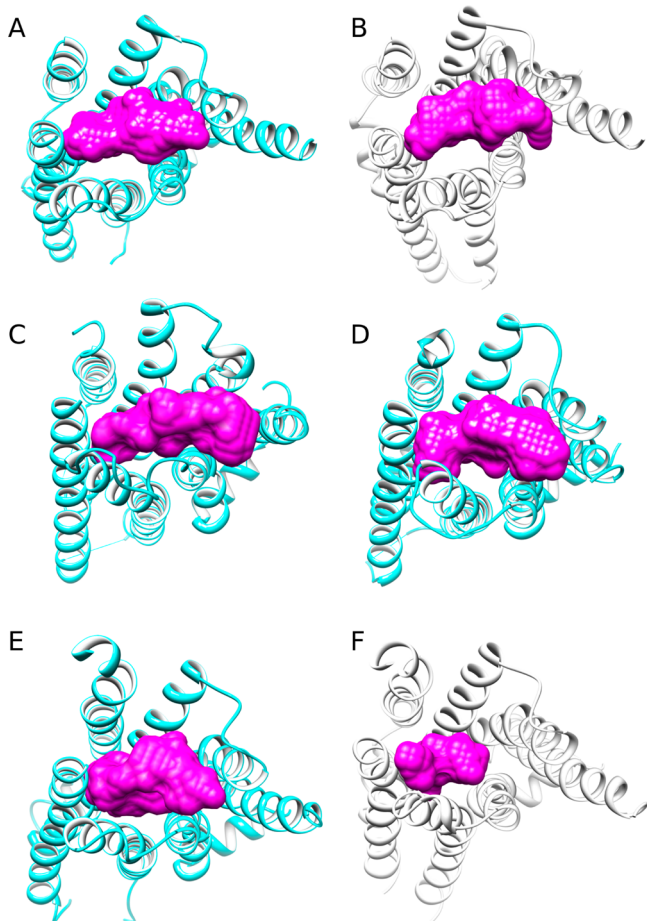


**Figure 9.** Binding-site volumes of Class A GPCR crystal structures, calculated with POVME.<sup>47</sup> Active-state GPCRs shown in light gray and inactive GPCRs in cyan. (A–B)  $\beta$ -2-adrenergic receptor with antagonist and agonist, respectively. (C) Sphingosine 1-phosphate receptor 1 with antagonist. (D) Dopamine D3 receptor with antagonist. (E, F) M2 muscarinic acetylcholine receptor with antagonist and agonist, respectively.

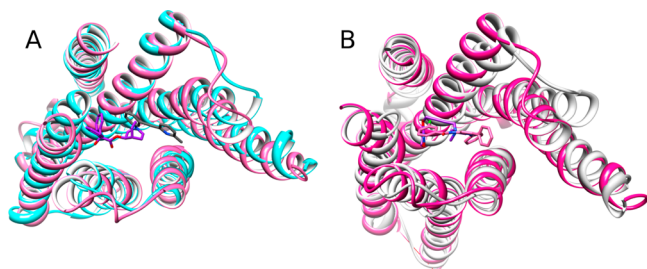


**Figure 10.** Structural comparison of mGluR5 with the crystal structures of the M2 muscarinic acetylcholine receptor (M2R). (A) Inactive state of mGluR5 (in cyan) with the inactive state of M2R (in light pink; PDB id, 3UON). (B) Active state of mGluR5 (in gray) with the active state of M2R (in dark pink; PDB id, 4MQS).

modeling and docking, NAMs and PAMs are observed to occupy the same allosteric pocket, although their exact binding modes and induced fit in the receptor differ. The models support the functional importance of W785 in the inactivation of the receptor based on direct interaction with NAMs, an interaction that is absent with PAMs in the activated receptor. In addition, the models reveal a set of core residues that are responsible for interacting with both PAMs and NAMs,

primarily located on TM3, TM6, and TM7. The residue N747 on TM5 is a notable exception, as it is observed to interact with 3-ring and 4-ring NAM/PAMs but not MPEP or VU0405386, which are both smaller 2-ring molecules. This result is supported by experimental data, which show N747 contributes to the binding affinity of VU0403602 but not VU0405386,<sup>27</sup> and 1,3-bisPEB but not MPEP.<sup>36</sup> This result can be explained by our models, which demonstrate 2-ring modulators do not reach as far into the pocket as 3-ring modulators, where N747 is predicted to be located.

MPEP is a particularly interesting allosteric modulator because it is the smallest of those docked here, and as a result has the freedom to explore binding modes that the other modulators do not. Although these other binding modes explored by MPEP are not as favorable as the top ranked solution found by ROSETTA, they may be viable alternatives should other allosteric modulators be docked at the same time.<sup>29,36</sup> This observation may explain the findings of other studies where MPEP and non-MPEP sites have been identified.<sup>52,53</sup> The modeling here shows that there is only one allosteric binding site, but this can perhaps be imagined as two “mini-pockets”, with MPEP potentially able to occupy one or the other or both. It can be speculated that a secondary MPEP binding mode may compete with the first but is nonfunctional in terms of negative allosterism (Figure 11).

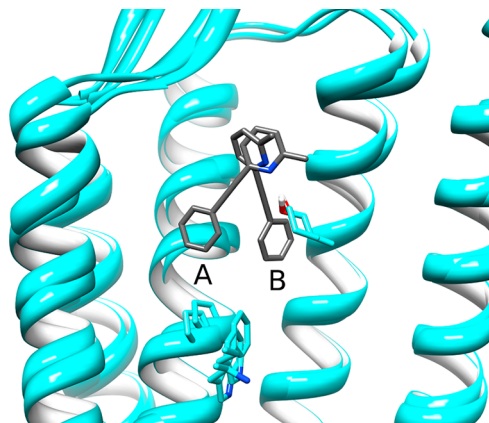


**Figure 11.** Primary (A) and secondary (B) binding modes of MPEP docked in mGluR5, displayed with CHIMERA<sup>41</sup> and viewed from within the membrane (TM6 and TM7 not shown), with side chains P655, W785, and S809 displayed.

Perhaps most significantly, the models here potentially explain the critical role of S809, and TM7 in general, in controlling both NAM and PAM function and receptor (in)activation. S809 has the capability to function as an “anchor” with all docked allosteric modulators and, depending on the point of anchoring with the modulator, causes either a positive or negative allosteric effect on the receptor. In turn, the interaction between allosteric modulator and S809 affects the orientation of TM7, which affects the shape of the allosteric pocket, as well as the orientation of TM6, potentially affecting the overall state of the receptor. The difference between mGluR5 PAMs and NAMs in some instances can be very subtle. A particularly good example is CHPyEPC and CHPhEPC, where changing one atom changes modulator chemical properties and, critically, changes the H-bond with S809. This change is facilitated by a rotation in the serine side chain and translocation of the TM7 backbone, which changes

the shape of the allosteric site. Furthermore, the flexible modeling implemented here reveals how PAMs docked into the inactive state of the receptor and NAMs docked into the active state, alter the allosteric site, suggesting a partial transition toward the other state. Such models may reflect an intermediary state, where the G-protein binding site on the intracellular side is still in an inactive state, while the allosteric site is induced into an activelike state, or indeed vice versa.

Molecular dynamics simulations can possibly be used to investigate communication between ligand binding site and G-protein binding site in GPCRs, as has been previously shown with B2AR, where two possible pathways were identified linking agonist/antagonist action to intracellular conformational changes.<sup>54</sup> These involved either the movement of TM6 or TM7 first, followed by movement of the other. Similar processes may happen in mGluR5, particularly as some of the structural features of TM6 and TM7 in B2AR are also present in mGluR5, e.g., WLxF motif in TM6 and FxPxxY motif<sup>55</sup> in TM7. However, such an investigation is beyond the scope of this study. Instead, we set out to demonstrate how flexible docking of allosteric modulators combined with a flexible receptor induces structural change that occurs during (in)-activation and that this, to some degree, is independent of the starting conformation of the receptor. Generating an induced fit between modulator and receptor is an important feature of accurate docking and is achieved here using ROSETTA, which operates with principles similar to molecular dynamics and allows for cycle-based adjustments of protein backbone, side chains, and ligand.<sup>46</sup> ROSETTA is a versatile tool that can be applied to *ab initio* protein folding,<sup>56</sup> structural refinement of homology models, and docking. It has recently been successfully applied to the study of several membrane proteins,<sup>57–59</sup> as well as specifically tested with GPCRs where the ROSETTA score was found to correlate with the most nativelike structures,<sup>60</sup> making it a suitable tool for use here.

Analyzing the overall shape of the allosteric site in mGluR5 reveals structural differences between active and inactive states, as well as between individual PAMs and NAMs themselves. PAMs create a tightening in the center of the allosteric site, with a widening at the end, while NAMs create a widening in the center and tightening at the end. These two allosteric-site shapes are distinctive and, despite some differences between the individual molecules, constitute a repeating trend in our mGluR5 models. This is interesting because some of these features are seemingly not inherited from the B2AR(a) templates and are instead a consequence of induced fit. However, the recently released active structure of the M2 muscarinic acetylcholine receptor displays similar changes in its binding site when compared to our active mGluR5 models, with a significant narrowing induced by an agonist.<sup>51</sup>

Describing possible activation mechanisms of Class C GPCRs by comparison to Class A GPCRs is a difficult task and relies on detailed modeling and experimental information. As such, we have employed state of the art modeling techniques combined with mutagenesis data to make the process as accurate as possible. Clearly there are limitations due to the low sequence similarity between Class A and Class C GPCRs. However, it is worth noting that sequence similarity between Class A GPCRs is often low also. For example, the Class A receptors, M2 muscarinic acetylcholine,  $\beta$ -2-adrenergic, and rhodopsin, share a sequence similarity of only 21–29%, yet show similar overall conformational change upon activation, resulting in rearrangement of the hydrophobic core.<sup>61</sup> This

indicates sequence alone does not confer GPCR function, but rather overall fold and carefully placed key structural features.<sup>61</sup> Therefore as sequence similarity between Class A and Class C GPCRs (16–20%) is not much lower than that between some Class A GPCRs, it is plausible that Class C GPCRs may share a common activation mechanism with Class A. Indeed, there are several regions of sequence similarity between the two families, which likely indicates key structural similarities (as structure is conserved to a greater degree than sequence<sup>62</sup>). These include, for example, the same amino acid bias on TM3 (enriched in Ser, Thr, Gly, and Ala), a conserved disulfide bridge connecting TM3 with TM5, a thin patch of conserved residues on TM1 reflecting its thin interhelical surface,<sup>63</sup> and two conserved sequence motifs on TM6 and TM7 mentioned previously.

In addition, experimental data suggest the mechanism of Class C GPCRs is similar to Class A. In particular, the truncated 7TM domain of mGluR5 (as well as other Class C GPCRs, e.g., GABA-B2<sup>64,65</sup> and Ca(2+)<sup>66</sup> receptors) has been shown to behave in a fashion identical to Class A GPCRs; i.e., the 7TM domain activated in response to PAM binding, acting as a classic agonist, and consequently binding G-protein. Conversely, the 7TM domain can be inactivated with a concomitant basal decrease in response to NAM binding, acting as an inverse agonist.<sup>10</sup> In another study, fluorescence resonance energy transfer (FRET) demonstrated that the activation-dependent 7TM conformational changes occurring in mGluR1 have a profile similar to Class A GPCRs.<sup>67</sup> Furthermore, a partial agonist of mGluR1 was shown to act slower than a full agonist, as previously seen in the Class A  $\alpha_{2A}$ -adrenergic receptor,<sup>68</sup> while 7TM activation was shown to take place within a time scale of approximately 50 ms, the same as many Class A GPCRs.<sup>67</sup>

Mutagenesis approaches have also identified mechanistic similarities between Class A and Class C GPCRs involved in receptor activation. The first of these studies identified a conserved “ionic lock” in Class C GPCRs that corresponds to the “ionic lock” formed between the E(D)RY motif on TM3 and D/E on TM6 in Class A GPCRs. Although the E(D)RY motif is absent in Class C GPCRs, two conserved residues, one helix turn higher on TM3 and TM6, respectively, perform a similar function.<sup>63</sup> For example, in the GABA-B2 receptor, residues K572 and D688 on TM3 and TM6, respectively, are thought to form the ionic lock, with mutation of either disrupting receptor function. Conversely, if these residues are swapped with one another, normal receptor functionality is restored.<sup>63</sup> In Class A GPCRs, the ionic lock stabilizes the inactive state and is broken when TM6 moves away from TM3 during receptor activation.<sup>33,69</sup> The authors conclude the same conformational change involving TM3–TM6 dissociation and concomitant ionic lock breakage occurs in Class C GPCRs<sup>63</sup> and interestingly is observed here in the modeling of mGluR5 (Figure 12).

A second mutagenesis study identified a water-mediated H-bonding network between TM6 and TM7 in the Class C GPCR mGluR8, which has previously been observed in Class A GPCRs.<sup>70–72</sup> The reorganization of this network facilitates receptor activation and specifically in mGluR8 involves the interaction of T789 (T6.43) on TM6 with the PxxY motif on TM7.<sup>70</sup> Likewise, in Class A GPCRs thyrotropin receptor and rhodopsin, loss of the H-bonding network between TM6 and NPxxY on TM7 increases receptor constitutive activity, particularly upon mutation of T6.43 and M6.40, respectively.<sup>73,74</sup> The authors conclude a similar structural rearrange-

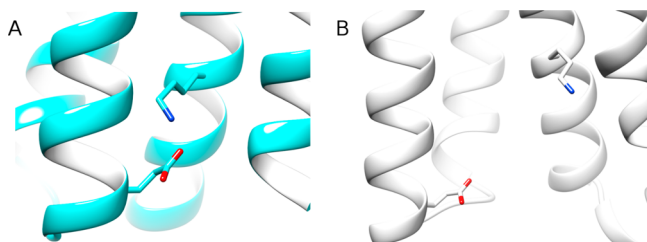


**Figure 12.** Comparison of the ionic lock (residues K665 and E770) in models of mGluR5: (A) “locked” inactive state (in cyan) and (B) “unlocked” active state (in gray).

ment between TM6 and TM7 is required for both Class A and Class C GPCR activation,<sup>70</sup> again, noted here in our models of mGluS (Figure 6).

Based on this accumulative evidence, it is reasonable to propose that the structural changes observed in Class A GPCR activation can be extended to Class C GPCRs and used as a basis of modeling. Indeed, as more active GPCR crystal structures are released, it is likely that the activation mechanisms observed in agonist/PAM binding will become clearer. Furthermore, more active-state GPCR crystal structures will aid in the construction of active-state Class C GPCR models, such as mGluR5, particularly through the use of multiple-template homology modeling.

Finally, recent studies have identified other residues that influence NAM and PAM activity in mGluR5, namely, Y659 (on TM3) and T781 (on TM6). In contrast with recent suggestions that these residues make direct ligand interactions, our models suggest these residues are located near the allosteric site but do not make direct contact with either PAMs or NAMs. Rather, Y659 and T781 are located beneath W785 and PAM/NAM, and our models suggest they are analogous to the “sliding microswitch” identified in Class A GPCRs, involving residues F6.44 and I3.40, which has a pivotal role in the transition between receptor states.<sup>75</sup> For activation to occur, these residues have to slide past each other. Our models suggest a similar mechanism in mGluR5, with changes in the orientation of W785 affecting the microswitch residues Y659 and T781.

## ■ CONCLUSION

Modeling Class C GPCRs from Class A GPCRs is a challenge because of their dissimilar sequences. Here we show that homology modeling based on a multiple sequence alignment between Class A and Class C members, followed by homology-guided docking and fully flexible ROSETTA receptor optimization, offers a suitable protocol for modeling the Class C GPCR mGluR5 with bound allosteric modulators. Modeling results suggest a common mechanism where both mGluR5 PAMs and NAMs elicit their effect via H-bonding with S809 on TM7, as well as NAMs exclusively interacting with W785. These specific interactions affect the overall shape of the allosteric site in a reproducible manner. Recently released crystal structures of the Class A GPCR M2 muscarinic acetylcholine receptor, in both active and inactive states, supports the hypothesis of structural changes in the binding site upon GPCR (in)activation, as observed here in the modeling of mGluR5.

## ■ ASSOCIATED CONTENT

### S Supporting Information

Figures showing multiple sequence alignment between mGluR5 and class A GPCR sequences and comparative alignment between mGluR5 models and a table listing mGluR5 residues involved in PAM/NAM docking. This material is available free of charge via the Internet at <http://pubs.acs.org>.

## ■ AUTHOR INFORMATION

### Corresponding Author

\*E-mail: jesus.giraldo@uab.es.

### Notes

The authors declare no competing financial interest.

## ■ ACKNOWLEDGMENTS

This study was supported in part by Ministerio de Economía y Competitividad (Grants SAF2010-19257 and ERA-NET NEURON PCIN-2013-018-C03-02) and Fundació La Marató de TV3 (Refs 110230 and 110231). We acknowledge the support of Generalitat de Catalunya (Grant 2009SGR-1072) and CSIC. Computations were performed in part at the Center for Scientific and Academic Services of Catalonia (CESCA).

## ■ ABBREVIATIONS

GPCR, G-protein coupled receptor; 7TM, heptahelical transmembrane; VFT, Venus flytrap; mGluR5, metabotropic glutamate receptor 5; PAM, positive allosteric modulator; NAM, negative allosteric modulator; ECL2, extracellular loop 2

## ■ REFERENCES

- Gregory, K. J.; Dong, E. N.; Meiler, J.; Conn, P. J. Allosteric modulation of metabotropic glutamate receptors: Structural insights and therapeutic potential. *Neuropharmacology* **2011**, *60*, 66–81.
- Niswender, C. M.; Conn, P. J. Metabotropic glutamate receptors: Physiology, pharmacology, and disease. *Annu. Rev. Pharmacol. Toxicol.* **2010**, *50*, 295–322.
- Featherstone, D. E. Intercellular Glutamate Signaling in the Nervous System and Beyond. *ACS Chem. Neurosci.* **2010**, *1*, 4–12.
- Nicoletti, F.; Bockaert, J.; Collingridge, G. L.; Conn, P. J.; Ferraguti, F.; Schoepp, D. D.; Wroblewski, J. T.; Pin, J. P. Metabotropic glutamate receptors: From the workbench to the bedside. *Neuropharmacology* **2011**, *60*, 1017–1041.
- Dingledine, R.; Borges, K.; Bowie, D.; Traynelis, S. F. The glutamate receptor ion channels. *Pharmacol. Rev.* **1999**, *51*, 7–61.
- Sugiyama, H.; Ito, I.; Hirose, C. A new type of glutamate receptor linked to inositol phospholipid metabolism. *Nature* **1987**, *325*, 531–533.
- Schoepp, D. D.; Jane, D. E.; Monn, J. A. Pharmacological agents acting at subtypes of metabotropic glutamate receptors. *Neuropharmacology* **1999**, *38*, 1431–1476.
- Mølck, C.; Harpsøe, K.; Gloriam, D. E.; Mathiesen, J. M.; Nielsen, S. M.; Bräuner-Osborne, H. mGluR5: Exploration of Orthosteric and Allosteric Ligand Binding Pockets and Their Applications to Drug Discovery. *Neurochem. Res.* **2014**, DOI: 10.1007/s11064-014-1248-8, (Feb 4 [Epub ahead of print]).
- Kniazeff, J.; Prézeau, L.; Rondard, P.; Pin, J. P.; Goudet, C. Dimers and beyond: The functional puzzles of class C GPCRs. *Pharmacol. Ther.* **2011**, *130*, 9–25.
- Goudet, C.; Gaven, F.; Kniazeff, J.; Vol, C.; Liu, J.; Cohen-Gonsaud, M.; Acher, F.; Prézeau, L.; Pin, J. P. Heptahelical domain of metabotropic glutamate receptor 5 behaves like rhodopsin-like receptors. *Proc. Natl. Acad. Sci. U. S. A.* **2004**, *101*, 378–383.
- Flor, P. J.; Acher, F. C. Orthosteric versus allosteric GPCR activation: The great challenge of group-III mGluRs. *Biochem. Pharmacol.* **2012**, *84*, 414–424.

- (12) Burford, N. T.; Watson, J.; Bertekap, R.; Alt, A. Strategies for the identification of allosteric modulators of G-protein-coupled receptors. *Biochem. Pharmacol.* **2011**, *81*, 691–702.
- (13) Conn, P. J.; Christopoulos, A.; Lindsley, C. W. Allosteric modulators of GPCRs: A novel approach for the treatment of CNS disorders. *Nat. Rev. Drug Discovery* **2009**, *8*, 41–54.
- (14) Conn, P. J.; Lindsley, C. W.; Jones, C. K. Activation of metabotropic glutamate receptors as a novel approach for the treatment of schizophrenia. *Trends Pharmacol. Sci.* **2009**, *30*, 25–31.
- (15) Swanson, C. J.; Bures, M.; Johnson, M. P.; Linden, A. M.; Monn, J. A.; Schoepp, D. D. Metabotropic glutamate receptors as novel targets for anxiety and stress disorders. *Nat. Rev. Drug Discovery* **2005**, *4*, 131–146.
- (16) Palucha, A.; Pilc, A. Metabotropic glutamate receptor ligands as possible anxiolytic and antidepressant drugs. *Pharmacol. Ther.* **2007**, *115*, 116–147.
- (17) Zhou, Q.; Wang, J.; Zhang, X.; Zeng, L.; Wang, L.; Jiang, W. Effect of metabotropic glutamate 5 receptor antagonists on morphine efficacy and tolerance in rats with neuropathic pain. *Eur. J. Pharmacol.* **2013**, *718*, 17–23.
- (18) During the review of this manuscript, the crystal structure of the 7TM domain of mGlu1 was released: Wu, H.; Wang, C.; Gregory, K. J.; Han, G. W.; Cho, H. P.; Xia, Y.; Niswender, C. M.; Katritch, V.; Meiler, J.; Cherezov, V.; Conn, P. J.; Stevens, R. C. Structure of a Class C GPCR Metabotropic Glutamate Receptor 1 Bound to an Allosteric Modulator. *Science* **2014**, *344* (6179), 58–64.
- (19) Fredriksson, R.; Lagerstrom, M. C.; Lundin, L. G.; Schioth, H. B. The G-protein-coupled receptors in the human genome form five main families. Phylogenetic analysis, paralogon groups, and fingerprints. *Mol. Pharmacol.* **2003**, *63*, 1256–1272.
- (20) Dalton, J. A.; Jackson, R. M. An evaluation of automated homology modelling methods at low target template sequence similarity. *Bioinformatics* **2007**, *23*, 1901–1908.
- (21) Kairys, V.; Fernandes, M. X.; Gilson, M. K. Screening drug-like compounds by docking to homology models: a systematic study. *J. Chem. Inf. Model.* **2006**, *46*, 365–379.
- (22) Dalton, J. A.; Jackson, R. M. Homology-modelling protein-ligand interactions: Allowing for ligand-induced conformational change. *J. Mol. Biol.* **2010**, *399*, 645–661.
- (23) Parmentier, M. L.; Prézeau, L.; Bockaert, J.; Pin, J. P. A model for the functioning of family 3 GPCRs. *Trends Pharmacol. Sci.* **2002**, *23*, 268–274.
- (24) Rovira, X.; Roche, D.; Serra, J.; Kniazeff, J.; Pin, J. P.; Giraldo, J. Modeling the binding and function of metabotropic glutamate receptors. *J. Pharmacol. Exp. Ther.* **2008**, *325*, 443–456.
- (25) Sams, A. G.; Mikkelsen, G. K.; Brodbeck, R. M.; Pu, X.; Ritzén, A. Efficacy switching SAR of mGluR5 allosteric modulators: Highly potent positive and negative modulators from one chemotype. *Bioorg. Med. Chem. Lett.* **2011**, *21*, 3407–3410.
- (26) Lindsley, C. W.; Wisnoski, D. D.; Leister, W. H.; O'Brien, J. A.; Lemaire, W.; Williams, D. L., Jr.; Burno, M.; Sur, C.; Kinney, G. G.; Pettibone, D. J.; Tiller, P. R.; Smith, S.; Duggan, M. E.; Hartman, G. D.; Conn, P. J.; Huff, J. R. Discovery of positive allosteric modulators for the metabotropic glutamate receptor subtype 5 from a series of *N*-(1,3-diphenyl-1*H*-pyrazol-5-yl)benzamides that potentiate receptor function *in vivo*. *J. Med. Chem.* **2004**, *47*, 5825–5828.
- (27) Gregory, K. J.; Nguyen, E. D.; Reiff, S. D.; Squire, E. F.; Stauffer, S. R.; Lindsley, C. W.; Meiler, J.; Conn, P. J. Probing the metabotropic glutamate receptor 5 positive allosteric modulator (PAM) binding pocket: Discovery of point mutations that engender a "molecular switch" in PAM pharmacology. *Mol. Pharmacol.* **2013**, *83*, 991–1006.
- (28) Cosford, N. D.; Tehrani, L.; Roppe, J.; Schweiger, E.; Smith, N. D.; Anderson, J.; Bristow, L.; Brodkin, J.; Jiang, X.; McDonald, I.; Rao, S.; Washburn, M.; Varney, M. A. 3-[(2-Methyl-1,3-thiazol-4-yl)-ethynyl]-pyridine: A potent and highly selective metabotropic glutamate subtype 5 receptor antagonist with anxiolytic activity. *J. Med. Chem.* **2003**, *46*, 204–206.
- (29) Kaae, B. H.; Harpsøe, K.; Kvist, T.; Mathiesen, J. M.; Mølck, C.; Gloriam, D.; Jimenez, H. N.; Uberti, M. A.; Nielsen, S. M.; Nielsen, B.; Bräuner-Osborne, H.; Sauerberg, P.; Clausen, R. P.; Madsen, U. Structure-activity relationships for negative allosteric mGluR5 modulators. *ChemMedChem* **2012**, *7*, 440–451.
- (30) Pagano, A.; Ruegg, D.; Litschig, S.; Stoehr, N.; Stierlin, C.; Heinrich, M.; Floersheim, P.; Prezeau, L.; Carroll, F.; Pin, J. P.; Cambria, A.; Vranesic, I.; Flor, P. J.; Gasparini, F.; Kuhn, R. The non-competitive antagonists 2-methyl-6-(phenylethynyl)pyridine and 7-hydroxyiminocyclopropan[b]chromen-1a-carboxylic acid ethyl ester interact with overlapping binding pockets in the transmembrane region of group I metabotropic glutamate receptors. *J. Biol. Chem.* **2000**, *275*, 33750–33758.
- (31) Malherbe, P.; Kratochwil, N.; Zenner, M. T.; Piussi, J.; Diener, C.; Kratzisen, C.; Fischer, C.; Porter, R. H. Mutational analysis and molecular modeling of the binding pocket of the metabotropic glutamate 5 receptor negative modulator 2-methyl-6-(phenylethynyl)-pyridine. *Mol. Pharmacol.* **2003**, *64*, 823–832.
- (32) Yanamala, N.; Tirupula, K. C.; Klein-Seetharaman, J. Preferential binding of allosteric modulators to active and inactive conformational states of metabotropic glutamate receptors. *BMC Bioinf.* **2008**, *9*, S1–S16.
- (33) Choe, H. W.; Kim, Y. J.; Park, J. H.; Morizumi, T.; Pai, E. F.; Krauss, N.; Hofmann, K. P.; Scheerer, P.; Ernst, O. P. Crystal structure of metarhodopsin II. *Nature* **2011**, *471*, 651–655.
- (34) Rasmussen, S. G.; DeVree, B. T.; Zou, Y.; Kruse, A. C.; Chung, K. Y.; Kobilka, T. S.; Thian, F. S.; Chae, P. S.; Pardon, E.; Calinski, D.; Mathiesen, J. M.; Shah, S. T.; Lyons, J. A.; Caffrey, M.; Gellman, S. H.; Steyaert, J.; Skiniotis, G.; Weis, W. I.; Sunahara, R. K.; Kobilka, B. K. Crystal structure of the  $\beta 2$  adrenergic receptor-Gs protein complex. *Nature* **2011**, *477*, 549–555.
- (35) Gregory, K. J.; Nguyen, E. D.; Malosh, C.; Mendenhall, J. L.; Zic, J. Z.; Bates, B. S.; Noetzel, M. J.; Squire, E. F.; Turner, E. M.; Rook, J. M.; Emmitt, K. A.; Stauffer, S. R.; Lindsley, C. W.; Meiler, J.; Conn, P. J. Identification of specific ligand–receptor interactions that govern binding and cooperativity of diverse modulators to a common metabotropic glutamate receptor 5 allosteric site. *ACS. Chem. Neurosci.* **2014**, *5*, 282–295.
- (36) Mølck, C.; Harpsøe, K.; Gloriam, D. E.; Clausen, R. P.; Madsen, U.; Pedersen, L. Ø.; Jimenez, H. N.; Nielsen, S. M.; Mathiesen, J. M.; Bräuner-Osborne, H. Pharmacological characterization and modeling of the binding sites of novel 1,3-bis(pyridinylethynyl)benzenes as metabotropic glutamate receptor 5-selective negative allosteric modulators. *Mol. Pharmacol.* **2012**, *82*, 929–937.
- (37) Bernstein, F. C.; Koetzle, T. F.; Williams, G. J.; Meyer, E. E., Jr.; Brice, M. D.; Rodgers, J. R.; Kennard, O.; Shimanouchi, T.; Tasumi, M. The Protein Data Bank: A Computer-Based Archival File for Macromolecular Structures. *J. Mol. Biol.* **1977**, *112*, 535–542.
- (38) Pei, J.; Kim, B. H.; Grishin, N. V. ProMALS3D: A tool for multiple protein sequence and structure alignments. *Nucleic Acids Res.* **2008**, *36*, 2295–2300.
- (39) Maestro, version 9.4; Schrödinger: New York, NY, 2013.
- (40) Banks, J. L.; Beard, H. S.; Cao, Y.; Cho, A. E.; Damm, W.; Farid, R.; Felts, A. K.; Halgren, T. A.; Mainz, D. T.; Maple, J. R.; Murphy, R.; Philipp, D. M.; Repasky, M. P.; Zhang, L. Y.; Berne, B. J.; Friesner, R. A.; Gallicchio, E.; Levy, R. M. Integrated Modeling Program, Applied Chemical Theory (IMPACT). *J. Comput. Chem.* **2005**, *26*, 1752–1780.
- (41) Pettersen, E. F.; Goddard, T. D.; Huang, C. C.; Couch, G. S.; Greenblatt, D. M.; Meng, E. C.; Ferrin, T. E. UCSF Chimera—A visualization system for exploratory research and analysis. *J. Comput. Chem.* **2004**, *25*, 1605–1612.
- (42) Hawkins, P. D.; Skillman, A. G.; Warren, G. L.; Ellingson, B. A.; Stahl, M. T. Conformer Generation with OMEGA: Algorithm and Validation Using High Quality Structures from the Protein Databank and the Cambridge Structural Database. *J. Chem. Inf. Model.* **2010**, *50*, 572–584.
- (43) Hawkins, P. D.; Skillman, A. G.; Nicholls, A. Comparison of Shape-Matching and Docking as Virtual Screening Tools. *J. Med. Chem.* **2007**, *50*, 74–82.
- (44) Ballesteros, J.; Weinstein, H. Integrated methods for the construction of three dimensional models and computational probing

- of structure-function relations in G protein coupled receptors. *Methods Neurosci.* **1995**, *25*, 366–428.
- (45) Sali, A.; Blundell, T. L. Comparative protein modelling by satisfaction of spatial restraints. *J. Mol. Biol.* **1993**, *234*, 779–815.
- (46) Misura, K. M.; Chivian, D.; Rohl, C. A.; Kim, D. E.; Baker, D. Physically realistic homology models built with ROSETTA can be more accurate than their templates. *Proc. Natl. Acad. Sci. U. S. A.* **2006**, *103*, 5361–5366.
- (47) Durrant, J. D.; de Oliveira, C. A.; McCammon, J. A. POVME: An algorithm for measuring binding-pocket volumes. *J. Mol. Graph. Model.* **2011**, *29*, 773–776.
- (48) Schwartz, T. W.; Frimurer, T. M.; Holst, B.; Rosenkilde, M. M.; Elling, C. E. Molecular mechanism of 7TM receptor activation—A global toggle switch model. *Annu. Rev. Pharmacol. Toxicol.* **2006**, *46*, 481–519.
- (49) Pellissier, L. P.; Sallander, J.; Campillo, M.; Gaven, F.; Queffeulou, E.; Pillot, M.; Dumuis, A.; Claeysen, S.; Bockaert, J.; Pardo, L. Conformational toggle switches implicated in basal constitutive and agonist-induced activated states of 5-hydroxytryptamine-4 receptors. *Mol. Pharmacol.* **2009**, *75*, 982–990.
- (50) Holst, B.; Nygaard, R.; Valentin-Hansen, L.; Bach, A.; Engelstoft, M. S.; Petersen, P. S.; Frimurer, T. M.; Schwartz, T. W. A conserved aromatic lock for the tryptophan rotameric switch in TM-VI of seven-transmembrane receptors. *J. Biol. Chem.* **2010**, *285*, 3973–3985.
- (51) Kruse, A. C.; Ring, A. M.; Manglik, A.; Hu, J.; Hu, K.; Eitel, K.; Hübner, H.; Pardon, E.; Valant, C.; Sexton, P. M.; Christopoulos, A.; Felder, C. C.; Gmeiner, P.; Steyaert, J.; Weis, W. I.; Garcia, K. C.; Wess, J.; Kobilka, B. K. Activation and allosteric modulation of a muscarinic acetylcholine receptor. *Nature* **2013**, *504*, 101–106.
- (52) Stauffer, S. R. Progress toward positive allosteric modulators of the metabotropic glutamate receptor subtype 5 (mGluR5). *ACS Chem. Neurosci.* **2011**, *2*, 450–470.
- (53) Wood, M. R.; Hopkins, C. R.; Brogan, J. T.; Conn, P. J.; Lindsley, C. W. “Molecular switches” on mGluR allosteric ligands that modulate modes of pharmacology. *Biochemistry* **2011**, *50*, 2403–2410.
- (54) Nygaard, R.; Zou, Y.; Dror, R. O.; Mildorf, T. J.; Arlow, D. H.; Manglik, A.; Pan, A. C.; Liu, C. W.; Fung, J. J.; Bokoch, M. P.; Thian, F. S.; Kobilka, T. S.; Shaw, D. E.; Mueller, L.; Prosser, R. S.; Kobilka, B. K. The dynamic process of  $\beta(2)$ -adrenergic receptor activation. *Cell* **2013**, *152*, 532–542.
- (55) Trzaskowski, B.; Latek, D.; Yuan, S.; Ghoshdastider, U.; Debinski, A.; Filipek, S. Action of molecular switches in GPCRs—Theoretical and experimental studies. *Curr. Med. Chem.* **2012**, *19*, 1090–1109.
- (56) Bonneau, R.; Baker, D. Ab initio protein structure prediction: Progress and prospects. *Annu. Rev. Biophys. Biomol. Struct.* **2001**, *30*, 173–189.
- (57) Dalton, J.; Kalid, O.; Schushan, M.; Ben-Tal, N.; Villà-Freixa, J. New model of cystic fibrosis transmembrane conductance regulator proposes active channel-like conformation. *J. Chem. Inf. Model.* **2012**, *52*, 1842–1853.
- (58) Li, F.; Xia, Y.; Meiler, J.; Ferguson-Miller, S. Characterization and modeling of the oligomeric state and ligand binding behavior of purified translocator protein 18 kDa from Rhodobacter sphaeroides. *Biochemistry* **2013**, *52*, 5884–5899.
- (59) Durdagi, S.; Deshpande, S.; Duff, H. J.; Noskov, S. Y. Modeling of open, closed, and open-inactivated states of the hERG1 channel: Structural mechanisms of the state-dependent drug binding. *J. Chem. Inf. Model.* **2012**, *52*, 2760–2774.
- (60) Nguyen, E. D.; Norn, C.; Frimurer, T. M.; Meiler, J. Assessment and challenges of ligand docking into comparative models of G-protein coupled receptors. *PLoS One* **2013**, *8*, e67302. <http://www.plosone.org/article/info%3Adoi%2F10.1371%2Fjournal.pone.0067302> (accessed March 26, 2014).
- (61) Tehan, B. G.; Bortolato, A.; Blaney, F. E.; Weir, M. P.; Mason, J. S. Unifying Family A GPCR Theories of Activation. *Pharmacol. Ther.* **2014**, *143*, 51–60.
- (62) Chothia, C.; Lesk, A. M. The relation between the divergence of sequence and structure in proteins. *EMBO J.* **1986**, *5*, 823–826.
- (63) Binet, V.; Duthey, B.; Lecaillon, J.; Vol, C.; Quoyer, J.; Labesse, G.; Pin, J. P.; Prézeau, L. Common structural requirements for heptahelical domain function in class A and class C G protein-coupled receptors. *J. Biol. Chem.* **2007**, *282*, 12154–12163.
- (64) Binet, V.; Goudet, C.; Brajon, C.; Le Corre, L.; Acher, F.; Pin, J. P.; Prézeau, L. Molecular mechanisms of GABA(B) receptor activation: New insights from the mechanism of action of CGP7930, a positive allosteric modulator. *Biochem. Soc. Trans.* **2004**, *32*, 871–872.
- (65) Binet, V.; Brajon, C.; Le Corre, L.; Acher, F.; Pin, J. P.; Prézeau, L. The heptahelical domain of GABA(B2) is activated directly by CGP7930, a positive allosteric modulator of the GABA(B) receptor. *J. Biol. Chem.* **2004**, *279*, 29085–29091.
- (66) Ray, K.; Tisdale, J.; Dodd, R. H.; Dauban, P.; Ruat, M.; Northup, J. K. Calindol, a positive allosteric modulator of the human Ca(2+) receptor, activates an extracellular ligand-binding domain-deleted rhodopsin-like seven-transmembrane structure in the absence of Ca(2+). *J. Biol. Chem.* **2005**, *280*, 37013–37020.
- (67) Hlavackova, V.; Zabel, U.; Frankova, D.; Bätz, J.; Hoffmann, C.; Prezeau, L.; Pin, J. P.; Blahos, J.; Lohse, M. J. Sequential inter- and intrasubunit rearrangements during activation of dimeric metabotropic glutamate receptor 1. *Sci. Signaling* **2012**, *5*, ra59. <http://stke.sciencemag.org/cgi/content/full/sigtrans;5/237/ra59> (accessed April 29, 2014).
- (68) Nikolaev, V. O.; Hoffmann, C.; Bünenmann, M.; Lohse, M. J.; Vilardaga, J. P. Molecular basis of partial agonism at the neurotransmitter alpha2A-adrenergic receptor and Gi-protein heterotrimer. *J. Biol. Chem.* **2006**, *281*, 24506–24511.
- (69) Flanagan, C. A. A GPCR that is not “DRY”. *Mol. Pharmacol.* **2005**, *68*, 1–3.
- (70) Yanagawa, M.; Yamashita, T.; Shichida, Y. Glutamate acts as a partial inverse agonist to metabotropic glutamate receptor with a single amino acid mutation in the transmembrane domain. *J. Biol. Chem.* **2013**, *288*, 9593–9601.
- (71) Angel, T. E.; Chance, M. R.; Palczewski, K. Conserved waters mediate structural and functional activation of family A (rhodopsin-like) G protein-coupled receptors. *Proc. Natl. Acad. Sci. U. S. A.* **2009**, *106*, 8555–8560.
- (72) Okada, T.; Fujiyoshi, Y.; Silow, M.; Navarro, J.; Landau, E. M.; Shichida, Y. Functional role of internal water molecules in rhodopsin revealed by X-ray crystallography. *Proc. Natl. Acad. Sci. U. S. A.* **2002**, *99*, 5982–5987.
- (73) Urizar, E.; Claeysen, S.; Deupi, X.; Govaerts, C.; Costagliola, S.; Vassart, G.; Pardo, L. An activation switch in the rhodopsin family of G protein-coupled receptors: The thyrotropin receptor. *J. Biol. Chem.* **2005**, *280*, 17135–17141.
- (74) Deupi, X.; Edwards, P.; Singhal, A.; Nickle, B.; Oprian, D.; Schertler, G.; Standfuss, J. Stabilized G protein binding site in the structure of constitutively active metarhodopsin-II. *Proc. Natl. Acad. Sci. U. S. A.* **2012**, *109*, 119–124.
- (75) Valentin-Hansen, L.; Holst, B.; Frimurer, T. M.; Schwartz, T. W. PheVI:09 (Phe6.44) as a sliding microswitch in seven-transmembrane (7TM) G protein-coupled receptor activation. *J. Biol. Chem.* **2012**, *287*, 43516–43526.